NUMERICAL SIMULATION OF TANGENTIAL SLOT SYNTHETIC JETS IN CHANNEL

Adriano Menezes da Silva, adrianosaoleo@gmail.com
Conrad Yuan Yuen Lee, conrady@unisinos.br
Universidade do Vale do Rio dos Sinos - UNISINOS

Abstract. *The use of components and electronic devices with high power or data processing capabilities causes great heat generation. This fact, associated to with the technological trend toward miniaturization creates large heat fluxes that must be removed from within the electronic component to ensure performance and durability. Conventional air-cooling systems of the "cooler" type have shown deficiencies in dealing with this large heat dissipation requirement since this techniques rely on a large enough volumetric flowrate of air. Synthetic jets can be applied either as an alternative or a supplementary aid to air-cooling systems. A synthetic jet is created by the oscillation of a membrane inside a cavity, which induces the ejection and suctioning of fluid through a narrow orifice. Fluid ejected from the cavity displaces far enough so that is not drawn back inside the cavity by the oscillatory movement of the membrane. The resulting jet plume has average velocity and jet growth similar to a steady jet but contain higher turbulence levels and mass entrainment at the edges. Consequently, synthetic jets can greatly enhance mixing and increase heat transfer from a surface. Much attention has been given to impacting configurations, in which the jet plume is directed normal to a heated surface for hotspot cooling. However, tangential configurations, in which the jet plume is directed to blow along a heated surface, are more suitable for electronic cooling where finned heat exchangers are used. Consequently the purpose of this study is to create a fully 3-D model of a tangential jet generator operating with a compressible fluid. Simulation results are validated against a classic steady channel flow and experimental results of a synthetic jet-driven mean channel flow.*

Keywords*: synthetic jets, turbulent channel flow, CFD*

1. INTRODUCTION

Synthetic jet generators are devices formed by a cavity sealed on one side by a plate with a small orifice and equipped on the other end with an oscillating membrane (Smith and Glezer, 1998; Iwana *et al.*, 2015; Xia and Zhong, 2012). The synthetic jet plume forms in the blowing phase of the membrane oscillation, as the flow separates on the external orifice lips into vortical structures. Under the appropriate combination of pulsing frequency and jet Reynolds number, as the membrane reverses oscillation, the ejected vortices displace far enough from the orifice and are not drawn back inside the cavity, which is then fed from fluid drawn along the external walls surrounding the orifice (Saffman, 1981; Auerbach, 1987). In this manner, continuous membrane oscillation results in a jet with mean momentum away from the orifice and with average properties similar to a steady jet. However, unlike a steady jet, the fluid in the external medium also feeds the cavity, foregoing the need for a supplementary source of mass.

Applications for synthetic jets vary, ranging from boundary layer mixing to electronic cooling. The latter case is of particular interest due to its potential to achieve much higher heat transfer rates than conventional air-cooling techniques that rely on fans and finned heat exchangers. This application of synthetic jets occurs in two basic configurations: impingement cooling or tangential cooling. In the case of impingement cooling, the synthetic jet is directed perpendicular or at a steep angle to a surface so that its plume impacts against the heated region. Etemoglu (2007) noted that synthetic jet impingement results in a substantial increase in heat transfer and mass exchange in a region containing the impact zone. This turbulence enhancing characteristic of vortical structures of impinging synthetic jets were also demonstrated in the work of Pavlova and Amitay (2006), which reported that a synthetic jet directed at a surface heated by a constant heat flux resulted in Nusselt numbers up to 3 times larger than an equivalent steady jet with the same orifice and jet Reynolds number. Similar increases in impingement cooling were observed in the work of Gillespie *et al.*(2006). In the case of tangential cooling, the synthetic jet blows along or over the heated region. When this configuration is placed at the mouth of a channel, Mahalingam and Glezer (2005) noted that the synthetic jets induced a mean flow downstream. Comparisons between synthetic jet actuators and conventional fans supplying low volumetric airflow showed that the synthetic jets were able to dissipate 20% to 40% more heat. A numerical study of incompressible fluid in a 2-D domain by Munhoz *et al.* (2012) obtained similar results, with a synthetic jet producing Nusselt numbers 42% a 122% larger than a mean turbulent channel flow of equivalent mean mass flow rate. Small scale, ultra-thin devices suitable for portable electronics were tested by de Bock *et al.* (2012) and found to produce 2 to 2.5 times the temperature drop compared to natural convection whether the device operated in an open or enclosed space. Similarly, Mahalingam *et al.* (2014) tested a coupled device 3 mm in height that produced two slot jets and also found it able to increase cooling capacity by a factor of 2 when compared to natural convection.

Despite the documented advantages of synthetic jets, further studies are still required to determine the optimum configuration and operating parameters that will result in the largest increase in heat transfer. Simulations of Munhoz *et* *al.* (2012) observed that a synthetic jet developed a thicker layer of vorticity along the heated surface when compared to a steady turbulent flow of equivalent mass flow. This indicated that turbulent mixing induced by the synthetic jet was the driving mechanism for the cooling gains. However, experiments by Trisch (2015) showed only small gains in temperature reduction when a synthetic jet was compared to a conventional cooler fan providing the same volumetric flow rate. While this could be attributed to the turbulence generated by the cooler fan, Trisch (2015) also noted that it was necessary to utilize a fan of hydraulic diameter 6.6 larger than the slot jet to generate the same volumetric flow rate. This suggests that another mechanism for the cooling performance of synthetic jets would be its effectiveness in generating a relatively large volumetric flow rate in a confined space.

The work presented here is part of a larger study to examine the cooling effect and physical mechanisms of heat transfer in tangential synthetic jets. To this end, it is necessary first to construct and validate a simulation of a slot jet directed to blow downstream in a channel. The geometry of this simulation is accurate with respect to the experiments of Trisch (2015) with a compressible fluid in a 3-D domain and including the jet-generator cavity.

2. SYNTHETIC JET GEOMETRY AND ANALYSIS PARAMETERS

2.1 Synthetic jet generator and channel geometry

The synthetic jet generator and channel geometry are based on the experiments of Trisch (2015) and is shown schematically in Figure 1. It consists of a cylindrical jet generator cavity connected to an L-shaped duct, which directs the fluid drawn in and out of the cavity to flow tangentially along the bottom surface of the channel where the heating elements are embedded. The channel is open on both extremities to allow the synthetic jet to induce a mean channel flow downstream. The relevant dimensions of the domain are shown in Figure 2. The generator cavity has a diameter D_m = 76 mm and height H_m = 12.4 mm. The L-shaped jet duct has a rectangular cross-section of height H_d = 6 mm and width W_d = 20 mm for a hydraulic diameter of D = 9.23 mm. The vertical segment of the duct leaving the generator cavity measures 26 mm in length while the horizontal segment measures 20 mm in length, for an overall throat length of L_d = 56 mm. The channel has an overall length of L_c = 300 mm, height H_c = 50 mm and width W_c = 20 mm. As seen in Figure 2, the exit plane of the synthetic jet is mounted with an entrance length L_e = 20 mm from the channel entrance. The jet duct at the channel entrance has a thickness H_s = 3 mm. Consequently the channel entrance has a height H_e = 41 mm while the channel exit has the same full height of 50 mm as the channel. The downstream channel direction is defined as the x-direction, the vertical direction is defined as the y-direction and the spanwise direction is defined as the w-direction.

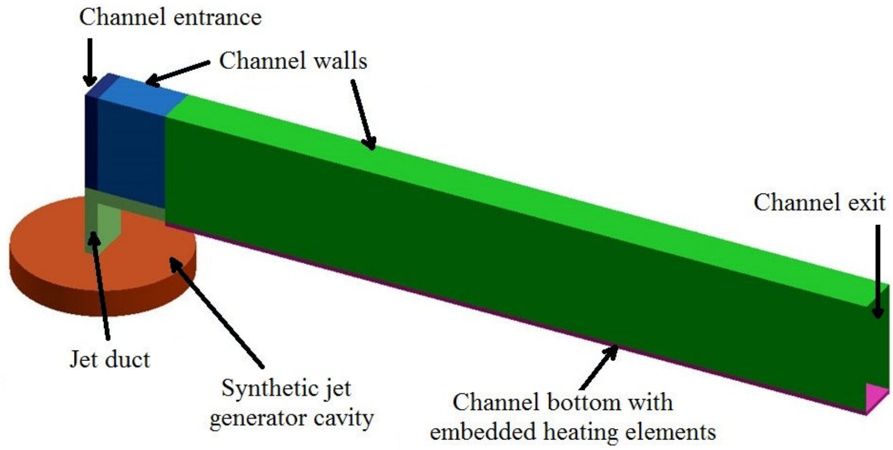

Figure 1. Diagram of synthetic jet generator and channel in the experiment of Trisch (2015)

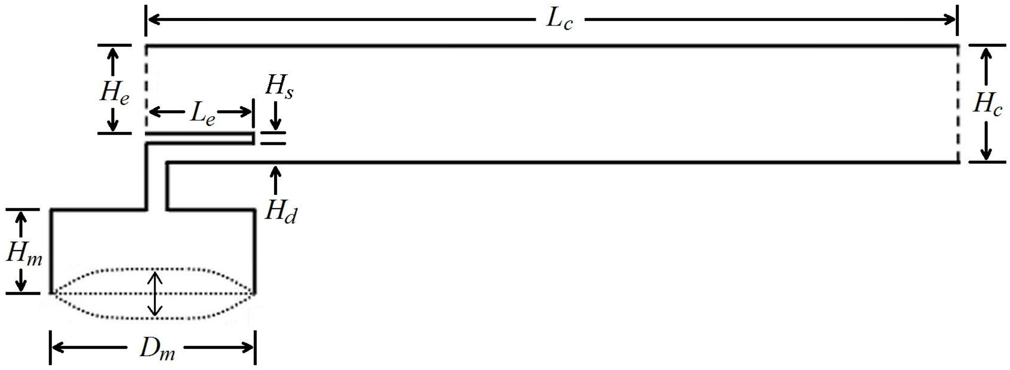

Figure 2: Schematic and relevant dimensions in the experiment of Trisch (2015)

2.2 Analysis Parameters

The main parameter of interest for the synthetic jet is the characteristic jet Reynolds number, given by Eq. (1):

$$Re_{jet} = \frac{\rho U_{jet} D}{\mu}, \tag{1}$$

where ρ is the fluid density, D is the jet orifice hydraulic diameter and μ is the fluid viscosity. The characteristic jet velocity, U_{jet}, is defined by Smith and Glezer (1998) as the average velocity at the jet exit plane over the blowing half-period of oscillation, as seen in Eq. (2):

$$U_{jet}(x) = \int_0^{T/2} u_{jet}(t)dt, \tag{2}$$

where T is the period of oscillation of the driving membrane in the cavity and $u(t)$ is the time-varying, spatially averaged flow velocity in the x-direction at a the jet exit plane.

Another parameter of interest for the synthetic jet is the characteristic jet Strouhal number, defined according to the characteristic jet velocity and orifice hydraulic diameter in Eq. (3):

$$St_{jet} = f \frac{D}{U_{jet}}, \tag{3}$$

where f is the oscillating frequency of the driving membrane in the cavity.

For a turbulent channel flow, the normalizing parameter of interest is the wall friction velocity, defined in Eq. (4):

$$u^* = \sqrt{\frac{\tau_w}{\rho}}, \tag{5}$$

where τ_w is the average wall shear stress given by Eq. (6):

$$\tau_w = \frac{1}{L} \int_0^L \tau_0(x)dx, \tag{6}$$

where τ_0 is the local wall shear stress.

3. NUMERICAL METHOD AND COMPUTATIONAL DOMAIN

3.1 Mathematical equations and turbulence modeling

A numerical approach is utilized in this study with the commercially available CFD software ANSYS CFX 15. The governing equations consist of the 3-D continuity and Navier-Stokes equations applied to a compressible fluid behaving as an ideal gas with constant thermal properties and no buoyancy. In Cartesian index notation, these are shown, respectively, in Eq. (7) and (8):

$$\frac{\partial \rho}{\partial t} + \frac{\partial (\rho U_i)}{\partial x_i} = 0 , \tag{7}$$

$$\frac{\partial (\rho U_i)}{\partial t} + U_j \frac{\partial (\rho U_i)}{\partial x_j} = -\frac{\partial P}{\partial x_i} + \frac{\partial \tau_{ij}}{\partial x_j} , \tag{8}$$

where t is the time, U_i is the instantaneous velocity field, x_i is a Cartesian direction, ρ is the density, P is the pressure field, and τ_{ij} is the deviatoric stress tensor given as a function of the velocity field and the dynamic viscosity by Eq. (9):

$$\tau_{ij} = \mu \left(\frac{\partial U_i}{\partial x_j} + \frac{\partial U_j}{\partial x_i} - \frac{2}{3} \partial_{ij} \frac{\partial U_i}{\partial x_i} \right). \tag{9}$$

Turbulent effects are considered through the two-equation Shear Stress Turbulence model (SST k-ω), which applies a blending function to automatically separate areas of the flow into zones where either the k-ε or k-ω model is applied. As noted by Menter *et al.* (2003), while the SST k-ω was initially developed for aeronautical applications with strong adverse pressure gradients and separation, its application has been extended for generic flows with pressure-induced separation when accurate solutions are desired.

The performance of the SST k-ω and other turbulence models for a steady straight round jet and a steady swirling round jet were examined by Miltner *et al.* (2015) and compared to experimental data. It was observed that all turbulence models yielded reasonable results for the straight jet centerline velocity decay. However, for the steady swirling jet, the velocities predicted by the SST k-ω and Reynolds Stress Model (RSM) were more accurate than the other models. The same result was also observed in turbulence intensity values along the jet centerline, although Miltner *et al.* (2015) noted that the calculated turbulence intensity in the near zone of the jet orifice tended to be under-predicted by all turbulence models due to insufficient turbulence development along the inside length of the jet throat. Radial jet profiles were also examined at several axial distances. For the straight jet, the SST k-ω and k-ε variants showed reasonable agreement with experimental data while the RSM and other models tended to over-predict lateral jet growth. Although the RSM mode presented good accuracy, Miltner *et al.* (2015) also noted that it was sensitive to the type of boundary condition and distance of its placement. Thus, although not as accurate as the RSM model, the SST k-ω model was less computational intensive and more robust, thus being the more recommended turbulence model for this type of flow.

3.2 Computational Mesh

To reduce the size of the computational mesh and time, an *x-y* symmetry plane is applied at the spanwise center of the channel and only half of the domain is considered. Additionally, in accordance to the study of Munhoz *et al.* (2012), a longer entry section is utilized to reduce the effects of a pressure boundary condition in the development of the jet plume. Thus, for the computational domain, L_e = 25 H_d and this longer entry section can be seen in the isometric view of Figure 3 and side view of Figure 4.

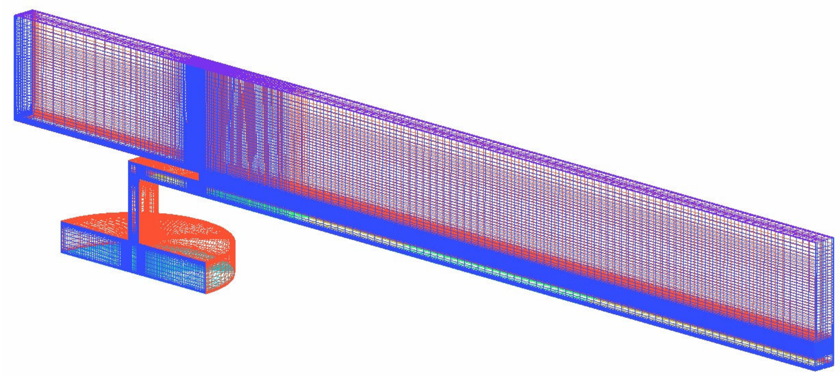

Figure 3. Isometric view of the computational domain used in this study

A side view of the symmetry plane showing the cavity region, L-shaped jet duct and entry region is displayed in Figure 4. As seen in the figure, grid refinement is applied near the channel walls in order to accurately resolve the momentum and thermal boundary layers. Additional refinement is also applied inside jet duct to capture correctly the oscillatory internal flow that develops. The study by Munhoz *et al.* (2012) identified that the region surrounding the jet exit to contain the largest gradients of velocity. Consequently, additional refinement is applied to a region of $\pm\ 2H_d$ centered at the jet exit plane.

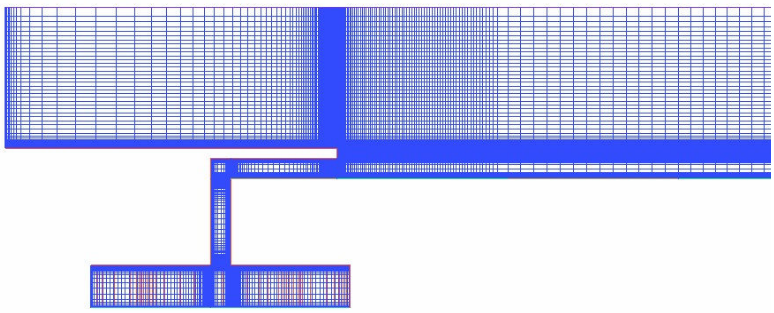

Figure 4. Side view detail showing cavity region, L-shaped jet duct and entry region with grid refinement

The minimum cell size was estimated by defining a cell-based Reynolds number, given by Eq. (11):

$$Re_{cell} = \frac{\rho U_{max} \Delta x_{cell}}{\mu}, \tag{11}$$

where U_{max} is the largest measured jet velocity and Δx_{cell} is the time smallest longitudinal cell spacing in the direction of the jet. The study by Munhoz *et al*. (2012) was conducted with a value of Re_{cell} = 0,386. Applying this value with the largest characteristic jet velocity measured in the experiments of Trisch (2015) allows the determination of the minimum cell spacing for this study, given by Eq. (12):

$$\Delta x = 0.386 \frac{\mu}{\rho U_{jet}}. \tag{12}$$

The mesh obtained according to this criterion was exceptionally fine. Therefore, a baseline mesh containing 50% of the number of elements is taken as the baseline grid of this study and validation tests were conducted on it

3.3 Membrane actuation

Membrane actuation has been represented in different forms in several numerical studies. Chandratilleke *et al.* (2010) opted to apply a sinusoidal time-varying moving boundary of constant amplitude, thus resembling a moving piston. Celik and Edis (2009) attempted to model the actual variation in shape of a moving membrane by applying a sinusoidal function in space. On the other hand, Xia *et al*. (2014) opted to apply a time varying velocity boundary condition of constant amplitude at the membrane location. Thus, no moving piston boundary exists but its transient velocity effect is represented in the cavity fluid. Similarly, Munhoz *et al*. (2012) and Lehnen *et al*. (2015) opted to simulate the effect of an actual flexible membrane by applying a sinusoidal-shaped, time-varying velocity profile at the membrane region.

Jain *et al.* (2011) studied the effect of modelling membrane actuation as a moving piston, moving shaped boundary or shaped velocity boundary condition. For each situation, the average longitudinal velocity at the jet exit plane is calculated over one period of actuation. Results show that while the velocity profile for the moving piston was distinct, with larger average velocities over the blowing part of the period, little difference is visible between a moving boundary or a velocity boundary. Thus, following the work of Munhoz *et al*. (2012) and Lehnen *et al*. (2015), a velocity boundary condition was selected for this study, given by Eq. (13):

$$U_m(r,t) = A_0 \cos\left(\frac{\pi}{D_m} r\right) \sin\left(\frac{2\pi t}{T}\right), \tag{13}$$

where U_m is the time and space-varying velocity in the membrane region of the computational domain, A_0 is a user-defined amplitude of velocity and r is the radial direction in the generator cavity.

4. RESULTS

4.1 Steady channel flow validation

The suitability of the baseline grid was tested with the synthetic jet turned off and a steady turbulent flow applied in the channel. The average mass flow rate through the channel was set to be identical to the highest value obtained by Trisch (2015). This value corresponds to a channel Reynolds number of 8,300. The resulting channel flow is similar to the classic backward-facing step flow problem in which the channel step height is given by $H = H_d + H_s$. For the baseline grid, the measured reattachment distance downstream of the step, normalized according to the step height was determined to be 7,7 H. This result is within 2.5% of the value obtained experimentally by Armaly *et al.* (1983), which corresponds to 7.9 H at a channel Reynolds number of 7,000. This confirms the suitability of the turbulence model and accuracy of the baseline grid.

The streamwise velocity profile is also taken at the *x-y* symmetry plane at the channel exit and shown in Figure 5. Results are normalized according to the friction velocity and compared to the theoretical universal turbulent boundary layer velocity profile. As seen in the figure, the baseline grid is refined enough to capture the near-wall viscous sublayer as well as the law of the wall. Consequently, the baseline grid resolution is also considered suitable to resolve the relevant physical phenomena of a turbulent boundary layer.

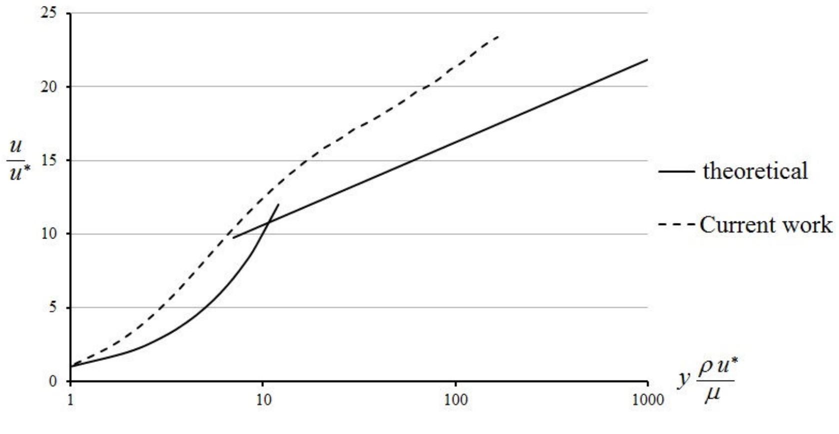

Figure 5. Velocity profile at the channel exit normalized according to wall units.

4.2 Synthetic jet-induced channel flow

The fully-developed steady turbulent channel flow velocity field was considered as the starting condition for the synthetic jet simulation. Channel entrance and exit boundary conditions were set to zero static pressure conditions so that there was no longer an external driving mechanism for the channel flow. Jet actuation was set to a pulsing frequency of 60 Hz (T = 0.0167 s) and an amplitude of velocity A_0 = 0.18 m/s. The resulting jet Reynolds number was calculated as 83.3 and the simulation was allowed to run through 180 pulses until the channel flow is considered to be stabilized.

The shear stress along the channel bottom for the current simulation is compared to the experimental results of Trisch (2015) in Figure 6. The values of shear stress have been normalized with respect to value measured with each case at a longitudinal position of $x/H_d = 10$. Results show that the wall shear stress from the current simulation has a similar decay rate the experimental values of Trisch (2015). This confirms that, in addition to a standard channel flow, the baseline grid is also accurate in representing turbulent flow phenomena induced by the synthetic jet.

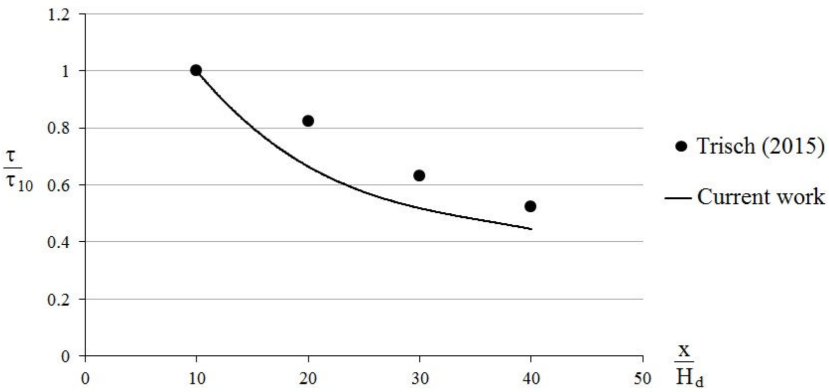

Figure 6. Comparison of normalized shear stress along the bottom channel surface.

The jet plume and evolution can be seen in the instantaneous contours of vorticity Ω_z at the *x-y* symmetry plane after the 180th pulse shown in Figure 7. Vorticity has been normalized according to the jet orifice hydraulic diameter (D) and average jet velocity (U_{jet}). As fluid is ejected from the L-shaped duct, the jet plume dissipates into the channel within 100 D. As the jet plume dissipates, it expands upwards into the channel and takes over as the driving mechanism for the mean channel flow, which reached a channel Reynolds of 5,600. As expected, boundary layers develop along both the top and bottom channel wall. However, interaction of the jet plume with the bottom channel wall up to a distance of 100 D indicates that within this region, higher turbulence levels and, by extension, enhanced heat transfer effects can be expected to occur.

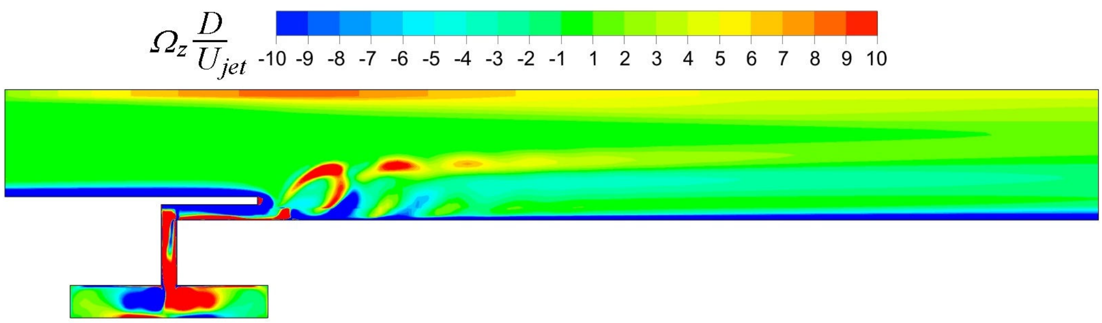

Figure 7. Normalized contours of instantaneous Ω_z vorticity after the 180th pulse.

5. CONCLUSIONS

A numerical simulation of a tangential synthetic jet has been developed based on the experiments of Trisch (2015). The numerical model considers a 3-D domain with an ideal gas with compressibility effects. The synthetic jet generator cavity and connecting duct are included in the model and membrane actuation is represented by a velocity boundary condition in lieu of an actual moving boundary. A baseline mesh is determined based on previous 2-D simulations and is validated with respect to the standard turbulent backwards-facing step problem. Results show that the baseline grid presents good agreement with respect to the reattachment length downsteam of the step and is refined enough to capture near-wall physical phenomena of a turbulent boundary layer. A synthetic jet-driven channel flow is tested and the wall shear stress decay along the surface shows good agreement with the experimental results of Trisch (2015). Contours of vorticity show that the jet plume expands into the channel dissipates within 100 D (hydraulic diameters) of the jet orifice and becomes the driving mechanism for the channel mean flow. Enhanced vortical structures are also observed within this 100 D region, suggesting that higher heat transfer effects are expected to occur within this region.

6. ACKNOWLEDGEMENTS

The authors would like to acknowledge the Unisinos Office of Research and Graduate Studies – UAPPG, Conselho Nacional de Desenvolvimento Científico e Tecnológico – CNPq and Instituto Tecnológico de Semicondutores da Unisinos – ittChip for their support.

7. REFERENCES

Armaly, G.F., Dursts, F., Pereira, J.C.F., Schonung, B., 1983. "Experimental and theoretical investigation of backward-facing step flow". *Journal of Fluid Mechanics*, Vol. 127, p. 473-496.

Auerbach, D., 1987. "Experiments on the trajectory and circulation of the starting vortex". *Journal of Fluid Mechanics*, Vol. 183, p. 185-198.

Celik, B., Edis, F.O., 2009. "Micro-scale synthetic-jet actuator flow simulation with characteristic-base-split method". *Aircraft Engineering and Aerospace Technology*, Vol. 81, No. 3, p. 239-246.

Chandratilleke, T.T., Jagannatha, D., Narayanaswamy, R., 2010. "Heat transfer enhancement in microchannels with cross-flow synthetic jets". *International Journal of Thermal Sciences*, Vol. 49, p. 504-513.

de Bock, H.P., Chamarthy, P., Jackson, J.L., Whalen, B., 2012. "Investigation and application of an advanced dual piezoelectric cooling jet to a typical electronics cooling configuration". In *Proceedings of the 13th IEEE ITHERM Conference*, San Jose, CA.

Etemoglu, A.K., 2007. "A brief survey and economical analysis of air cooling for electronic equipments". *International Communications in Heat and Mass Transfer*, Vol. 34, p. 103-113.

Gillespie, M.B. Black, W.Z., Rinehart, C., Glezer, A., 2006. "Local convective heat transfer from a constant heat flux at plate cooled by synthetic air jets". *Journal of Heat Transfer*, Vol. 128, No. 10, p. 990-1000.

Iwana, T., Suenaga, K., Shirai, K., Kameya, Y., Motosuke, M., Honami, S., 2015. "Heat transfer and fluid flow characteristics of impinging jet using combined device with triangular tabs and synthetic jets". *Experimental Thermal and Fluid Science*, Amsterdan, No. 68, p. 322-329.

Jain, M., Puranik B., Agrawal A., 2011. "A numeral investigation of effects os cavity and orifice parameters on the characteristics of a synthetic jet flow". *Sensors and Actuators A: Physical*. Vol. 165, No. 2, p. 351-366.

Lehnen, M.V., Lee. C.Y.Y., Alves, F.L.D., 2015. "Nusselt number correlation for synthetic jets". *Journal of the Brazilian Society of Mechanical Sciences and Engineering, Online first articles*, doi: 10.1007/s40430-015-0337-1.

Mahalingam, R., Poynot, A., Helsel, J., 2014. "Ultrathin synthetic jets for thermal management of consumer electronics". In *Proceedings of the 30th Semiconductor Thermal Measurement & Management Symposium (SEMI-THERM)*, San Jose, CA.

Mahalingam, R., Glezer, A., 2005. "Design and thermal characteristics of a synthetic jet ejector heat sink". *Journal of Electronic Packaging*, No. 127, p. 172-177.

Miltner, M., Jordan, C., Harasek, M. 2015. "CFD simulation of straight and slightly swirling turbulent free jets using different RANS-turbulence models". *Applied Thermal Engineering*, Vol. 89, p 1117-1126, doi:10.1016/j.applthermaleng.2015.05.048.

Menter, F.R., Kuntz, M., Langtry R., 2003. "Ten years of industrial experience with the SST turbulence model". *Turbulence, Heat and Mass Transfer 4: Proceedings of the Fourth International Symposium on Turbulence, Heat and Mass Transfer*, Antalya, Turkey.

Munhoz, F., Lee, C. Y. Y., Alves, F. L. D., 2015. "Numerical study of cooling by tangential synthetic jet". *Engenharia Térmica (Thermal Engineering)*, Vol. 14, No. 1, p. 47-53.

Pavlova, A., Amitay, M., 2006. "Electronic cooling using synthetic jet impingement". *Journal of Heat Transfer*, Vol. 128, No. 9, p. 897-907.

Saffman, G., 1981. "Dynamics of vorticity". *Journal of Fluid Mechanics*, Vol. 106, p. 49-58.

Smith, B.L., Glezer, A., 1998. "The formation and evolution of synthetic jets". *Physics of Fluids*, Vol. 10, No. 9, p. 2281-2297.

Trisch, M., 2015. "Resfriamento de componentes eletrônicos por jatos sintéticos tangenciais". *Dissertação Mestrado. Programa de Pós-Graduação em Engenharia Mecânica*, Universidade do Vale do Rio dos Sinos, São Leopoldo.

Xia, Q.. Lei, S., Ma, J., Zhong, S., 2014. "Numerical study of circular jets at low Reynolds numbers". *International Journal of Heat and Fluid Flow*, Vol. 50, p. 456-466.

Xia, Q., Zhong, S., 2012. "An experimental study on the behaviours of circular synthetic jets at low Reynolds numbers". *Proc. Institut. Mechan. Eng., Part C: Journal of Mechanical Engineering Science*. Vol. 226, p. 2686–2700.

8. RESPONSIBILITY NOTICE

The authors are the only responsible for the printed material included in this paper.